1

RESEARCH ARTICLE

Investigation of Flexural Capacity of Normal and Recycled Aggregate Concrete Filled Steel Tubes

Ma'en Abdel-Jaber[1], Mutasim Abdel-Jaber[2], Rola El-Nimri[3] and Hasan Katkhuda[4,*]

[1]*Department of Civil Engineering, School of Built Environment Engineering, Al Hussein Technical University, Amman, Jordan*
[2]*Department of Civil Engineering, Al-Ahliyya Amman University, Amman, Jordan*
[3]*Department of Civil Engineering, University of Jordan, Amman, Jordan*
[4]*Department of Civil Engineering, Faculty of Engineering, The Hashemite University, P.O. Box 330127, Zarqa 13133, Jordan*

Abstract:

Aims:

This paper aims to compare the experimental and theoretical results of the flexural capacity of normal and recycled aggregate concrete-filled tubes (CFT).

Background: The experimental results of 47 CFT specimens made of natural aggregate (NA), recycled concrete aggregate (RCA), and recycled asphalt pavement (RAP) with steel thicknesses of 2 and 2.4 mm from previous research performed by the authors are adopted.

Methods:

The NA was replaced in the CFT specimens by RCA and RAP with replacement levels of 20%, 40%, 60%, 80%, and 100%. The theoretical study is conducted in this paper based on the provisions of many international codes, available models from the literature, and finite element analysis (FEA) using Abaqus software to obtain the best approach for determining the flexural capacity of CFT.

Results:

The results showed that all code provisions were safe to use as they provided conservative results except for the ACI 318-19. The ANSI/AISC 360-16 and CoPHK provided the best conservative and accurate results.

Conclusion:

Besides, the finite element analysis results were found in good agreement with the experimental results as they provided the most accurate estimation.

Keywords: Flexural strength, Concrete filled tubes (CFT), Moment capacity, Finite element analysis (FEA), Recycled aggregate, Experimental and theoretical studies.

1. INTRODUCTION

Concrete filled tubes (CFT) have been the focus of recent research due to the advantages they provide to the construction industry [1 - 18]. The composite action between the steel and concrete infill helps to enhance the characteristics of each element. The steel tube provides triaxial confinement to the concrete infill that improves the concrete strength, which permits using different kinds of concrete such as normal con-crete, foamed and lightweight concrete, recycled aggregate concrete, and fly ash, quarry waste and low strength concrete. On the other hand, concrete enhances the steel characteristics by filling the inside void and preventing steel buckling, which improves the structural capacity.

Flor *et al.* [19] conducted an experimental study on the flexural behavior of large-scale rectangular CFT beams. Two 12 m long specimens were tested under two different methods to pour the concrete into the tubes and six 6 m long beams were tested under pure bending. The ultimate moment capacity was determined based on the plastic stress distribution with all

* Address correspondence to this author at the Department of Civil Engineering , Faculty of Engineering, The Hashemite University, P.O. Box 330127, Zarqa 13133, Jordan; Tel: 00962796491001; E-mail: hasan@hu.edu.jo

safety factors set to unity. Results proved that for the tested CFT beams, the predicted moment capacity was about 2% higher than the experimental flexural capacity. Xiong *et al.* [20] investigated the flexural performance of CFT with high tensile steel and ultra-high strength concrete. A total of eight circular, square, single-tube, and double-tube CFSTS were adopted. Results showed that the estimation of the flexural capacity according to the euro code (EC4) could be safely extended to ultra-high strength concrete by considering a reduction factor. Nghiem *et al.* [21] investigated the flexural performance of circular concrete-filled tubes without axial forces and conducted a comparison using the calculated and measured moment strength of CFT of the current and previous experiments. A total of five specimens were considered in their program, including four CFTS. Theoretical capacities were estimated by using ACI, AISC, and Eurocode 4 equations. All codes predicted the moment strength of CFT beams reasonably well, in which the ACI is the most conservative one among the three codes. Javed *et al.* [22] conducted a finite element analysis of the flexural behavior of square CFT at ambient and elevated temperature using ANSYS software. The model was verified with the experimental results from previous studies. It was found that the developed FE model can accurately predict the moment capacity of the square CFT beams subjected to flexural loads and fire resistance time, where the load-deflection curves and the ultimate moment capacity were found in a reasonable agreement with the experimental results. El-Nimri R. [23] investigated the flexural behavior of light-gauge steel box sections filled with normal and recycled aggregate concrete under a four-point loading test. A total of forty-seven beams were tested. The experimental results showed that the flexural capacity of CFT beams decreased with the increase of RCA and RAP percentage.

Although prediction of the flexural strength of CFT has been highlighted in several previous research using different codes; there are no clear conclusions on the best approach for determining the flexural capacity of CFT.

In this paper, the experimental results of 47 CFT specimens made of natural aggregate (NA), recycled concrete aggregate (RCA), and recycled asphalt pavement (RAP) with steel thickness of 2 and 2.4 mm from previous research [23] performed by the authors are adopted. The NA was replaced in the CFT specimens by RCA and RAP with replacement levels of 20%, 40%, 60%, 80%, and 100%. The experimental results are compared with the theoretical results from different international codes such as: Building Code Requirements for Structural Concrete (ACI 318-19) [24], Eurocode 4: Design of composite steel and concrete structures (EC4) [25], Specification for Structural Steel Buildings (ANSI/AISC 360-16) [26], Load and resistance factor design specification for structural steel buildings (AISC-LRFD 1999) [27], Recommendations for the design and construction of concrete filled steel tubular structures (AIJ 1997) [28], British Standards for steel, concrete, and composite bridges (BS 5400-5:1979) [29], the rigid plastic theory (RPT) [30], Code of Practice for the Structural Use of Steel 2005 (CoPHK) [31], and the proposed method by Han [5]. Moreover, the experimental results were compared with the finite element analysis (FEA) results by using Abaqus software to obtain the best approach

for determining the flexural capacity of CFT.

2. THEORETICAL STUDY USING CODES AND MODELS

2.1. ACI 318-19

The ACI 318-19 code [24] assumes that the maximum strain at the extreme concrete compression fiber ε_c equals 0.003, while the tensile strength is neglected. Moreover, a uniformly distributed stress of $0.85f_c$ is assumed over an equivalent compression zone bounded by edges of the cross-section and a line parallel to the neutral axis located distance (a) from the fiber of maximum compressive strain, as calculated by $a = \beta_1 c$, where c is the perpendicular distance from the most compressed fiber to the neutral axis, β_1 is a factor relating the depth of equivalent rectangular compressive stress block to depth of neutral axis, and f_c is the specified compressive strength of concrete.

Furthermore, the ACI 318-19 assumes that the reinforcement stress is proportional for strain below the specified yield strength f_y. Fig. (**1**) illustrates the stress distribution along the cross section according to the ACI 318-19.

2.2. EUROCODE 4

The EC4 [25] assumes the full interaction between steel and concrete, in which the effective area of concrete in compression resists a constant stress of $0.85f_{cd}$ over the whole depth between the plastic neutral axis and the most compressed fiber of the concrete, where f_{cd} is the design cylinder compressive strength. On the other hand, the steel is stressed to its design yield strength f_{yd} in tension or compression. Fig. (**2**) illustrates the stress distribution along the cross section according to the EC4.

2.3. ANSI/AISC 360-16

The nominal strength of composite sections is calculated based on either the plastic stress distribution method, the strain compatibility method, the elastic stress distribution method, or the effective stress-strain method.

2.3.1. Plastic Stress Distribution Method (PSDM)

The steel is assumed to reach its yield stress (F_y) in tension and compression, and the concrete in compression is stressed to $0.85f_c$ due to axial force or flexure, where f_c is the specified compressive strength of concrete. For round hollow structural steel (HSS), concrete, compression stress of $0.95f_c$ can be used because of concrete confinement. Fig. (**3**) provides an illustration of the stress distribution according to PSDM method.

2.3.2. Strain Compatibility Method (SCM)

Across the section, a linear strain distribution is assumed with the strain of concrete at the maximum compressed compression fiber equals 0.003.

2.3.3. Elastic Stress Distribution Method

The nominal strength is determined from the superposition of elastic stresses in the limit state of yielding or concrete crushing.

2.3.4. Effective Stress-Strain Method

In this method, the nominal strength is calculated assuming strain compatibility and effective stress-strain relationships for steel and concrete components considering the effects of local buckling, yielding, interaction, and concrete confinement.

2.4. AISC-LRFD (1999)

The AISC-LRFD [27] provisions assume that the moment capacity of hollow structural steel beams filled with concrete depends only on the steel section alone. Thus, the ultimate moment of resistance is assumed to be calculated based on a full plastic stress distribution on the steel section without any contribution from concrete. The stress distribution along the cross section according to the AISC-LRFD is shown in Fig. (**4**).

2.5. AIJ

The AIJ code [28] provisions assume that when calculating the ultimate moment of resistance of a concrete-filled tube member, each of the steel and concrete infills develops their individual plastic strengths, without accounting for the compatibility between steel and concrete. For members subjected to pure flexural load, the ultimate moment of resistance is calculated based on a full plastic stress distribution on the steel section alone, which is the same method used in the AISC-LRFD. Fig. (**5**) illustrates the stress distribution along the cross section according to the AIJ.
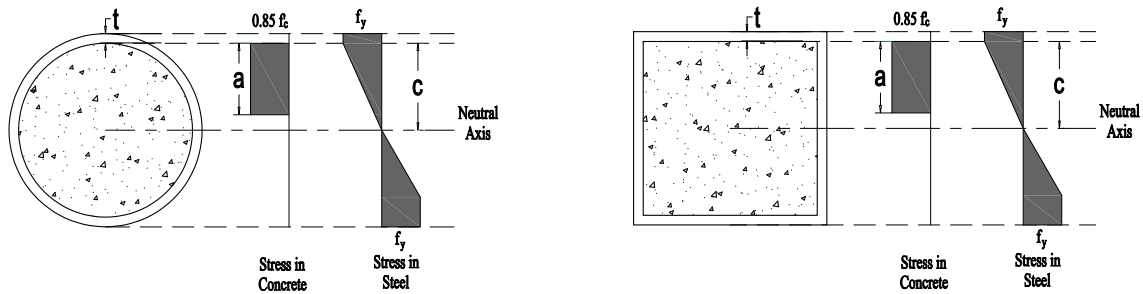

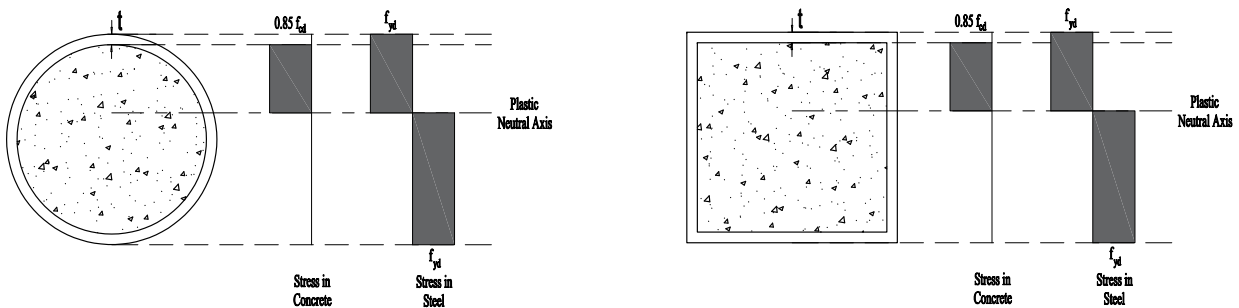**Fig. (1).** Stress distribution along the section according to ACI 318-19.

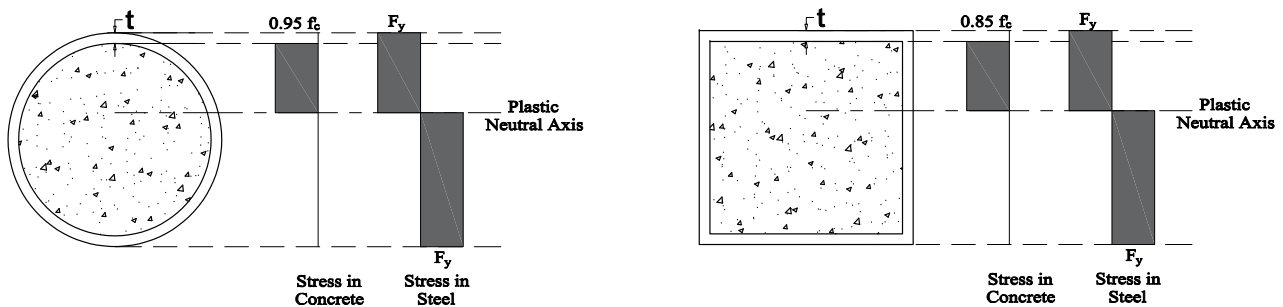**Fig. (2).** Stress distribution along the section according to EC4.

Fig. (3). Stress distribution along section according to ANSI/AISC 360-16/PSDM.

Fig. (4). Stress distribution along section according to AISC-LRFD (1999).

2.6. BS 5400-5:1979

BS 5400-5 [29] assumes the concrete stress in compression equal to $\frac{0.67 \times f_{cu}}{\gamma_{mc}}$ over the whole compression zone, where f_{cu} is the characteristic concrete cube strength and γ_{mc} is a partial safety factor for strength and is equal to 1.5. In the case of rectangular sections and flanged, ribbed, and voided sections where the neutral axis lies within the flange, the concrete compressive stress may be taken as $0.4f_{cu}$. In both cases, the strain at the maximum compression fiber at failure is 0.0035.

Stresses in steel in both tension and compression equals $\frac{0.8 \times f_y}{\gamma_{ms}}$, , where f_y is the characteristic strength of reinforcement and γ_{ms}

is a partial safety factor for strength and equals 1.15. Fig. (**6**) illustrates the stress distribution along the cross section according to the BS 5400-5.

2.7. Rigid Plastic Theory (RPT)

Rigid plastic analysis theory [30] is used to calculate the moment capacity for concrete-filled steel tubes. The flexural strength is obtained by determining the force distribution of both the steel and concrete individually and introducing the interaction between the steel and concrete by a bond force. Fig. (**7**) illustrates the stress distribution along the cross section according to the RPT.
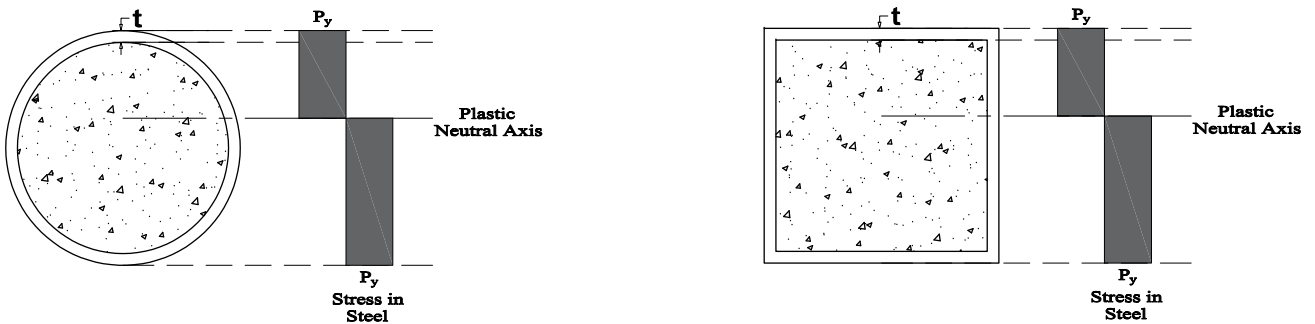
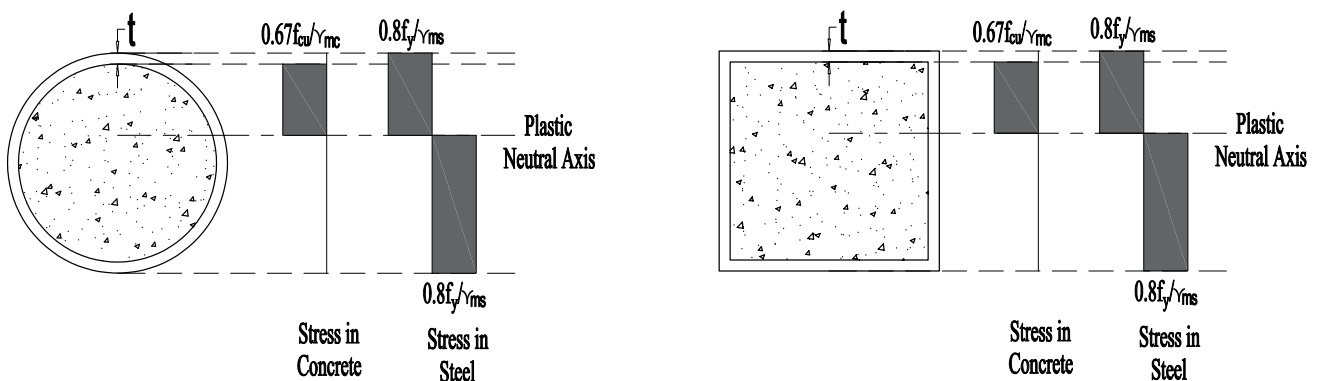**Fig. (5).** Stress distribution along the section according to AIJ.

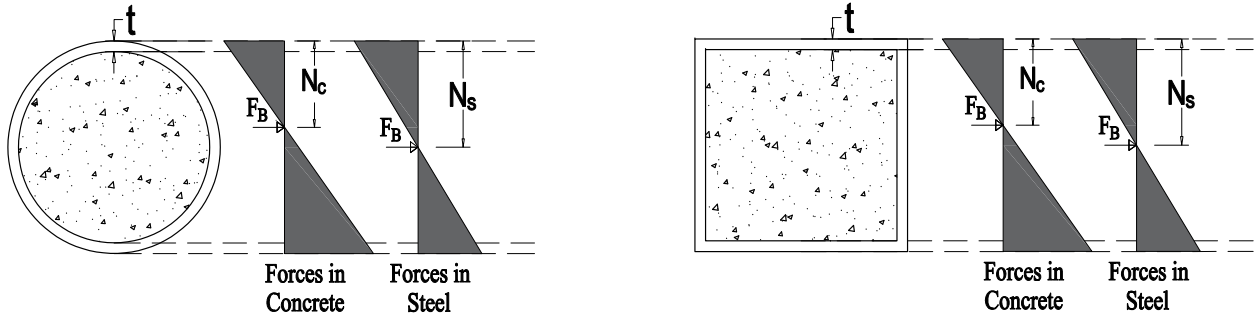**Fig. (6).** Stress distribution along the section according to BS 5400-5:1979.

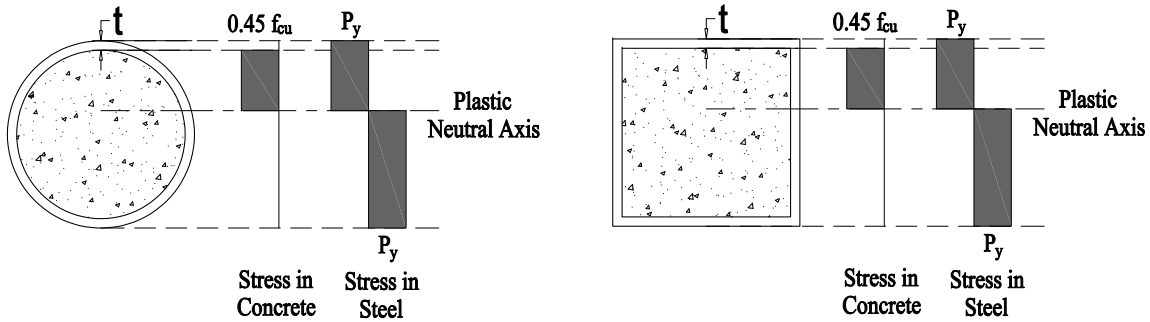**Fig. (7).** Stress distribution along the section according to RPT.

Fig. (8). Stress distribution along the section according to CoPHK.

2.8. Code of Practice for the Structural Use of Steel 2005 (CoPHK)

The plastic moment capacity is calculated according to the assumption of concrete is stressed to $0.45f_{cu}$ over the whole depth from the most compressed fiber to the plastic neutral axis, where f_{cu} is the cube compressive strength of concrete. On the other hand, the structural steel is stressed to its designed yield stress of P_y either in tension or compression. Fig. (**8**) illustrates the stress distribution along the cross section according to the CoPHK [31].

2.9. The Proposed Method by Han

Han 2004 [5] defines the flexural strength as:

$$(M_u = \gamma_m \times W_{scm} \times f_{scy}) \qquad (1)$$

where:

M_u is the moment capacity of the composite beams.

f_{scy} is the nominal yielding strength of the composite sections, given by:

• $f_{scy} = (1.18 + 0.85\ \xi) \times f_{ck}$ for square and rectangular sections

• $f_{scy} = (1.14 + 1.02\ \xi) \times f_{ck}$ for circular sections

W_{scm} is the section modulus of the composite beam, given by:

• $B^3/6$ for composite beams with square sections

• $BD^2/6$ and $B^2D/6$ about major (x–x) and minor (y–y) axes, respectively, for composite beams with rectangular

sections

• $(\pi D^3)/32$ for composite beams with circular sections

γ_m **is a** flexural strength index, given by:

• $\gamma_m = 1.04 + 0.48\ \ln(\xi + 0.1)$ for square and rectangular sections

• $\gamma_m = 1.1 + 0.48\ \ln(\xi + 0.1)$ for circular sections

ξ is a confinement factor equal to

$$\xi = \frac{A_s \times f_{sy}}{A_c \times f_{ck}},$$

Where A_s is the cross-sectional area of the steel tube, A_c is the cross-sectional area of the concrete core, f_{sy} is the yield stress of the outer steel tube, and f_{ck} is the compression strength of concrete in which for normal strength concrete is determined using 67% of the compression strength of cubic blocks.

3. MATERIALS AND METHODS

A set of previous tests performed by El-Nimri *et al.* [23] were used to measure the accuracy of the existing code provisions. The samples were light-gauge steel beams filled with NA, RCA, and RAP. The NA was replaced by RCA and RAP with different replacement levels of 0%, 20%, 40%, 60%, 80%, and 100% by weight. In addition, RCA and RAP were incorporated in the same mixes with four replacement levels of (20% RCA and 80% RAP); (40% RCA and 60% RAP); (60% RCA and 40% RAP); and (80% RCA and 20% RAP). The mass, density, and compressive strength for all concrete mixes are illustrated in Table **1**.

Table 1. Mass, density, and compressive strength of concrete mixes.

Mix Number	Mass (kg)	Density (kg/m^3)	f$_{cu}$ at 7 Days (MPa)	f$_{cu}$ at 28 Days (MPa)	Relative f$_{cu}$
Control Mix	8.44	2501.16	23.41	37.62	0.62
20% RCA + 80% NA	8.04	2382.32	19.75	32.36	0.61
40% RCA + 60% NA	7.84	2322.72	16.14	29.04	0.56
60% RCA + 40% NA	7.80	2310.86	16.99	30.09	0.57
80% RCA + 20% NA	7.87	2330.86	17.80	27.946	0.64
100% RCA	7.59	2247.7	13.42	20.83	0.64
20% RAP + 80% NA	8.04	2383.49	20.47	27.96	0.73
40% RAP + 60% NA	7.84	2323.75	16.89	26.94	0.63
60% RAP + 40% NA	7.81	2314.37	19.73	26.96	0.73
80% RAP + 20% NA	7.66	2269.63	16.36	25.14	0.65
100% RAP	7.51	2225.93	17.99	23.02	0.78
20% RCA + 80% RAP	7.57	2242.12	17.78	23.24	0.77
40% RCA + 60% RAP	7.68	2274.57	15.27	21.81	0.70
60% RCA + 40% RAP	7.65	2265.98	17.65	21.89	0.81
80% RCA + 20% RAP	7.69	2279.44	18.09	27.74	0.65

The composite beams had two steel thicknesses of 2 mm and 2.4 mm. Fifteen composite specimens of each steel thickness were considered, producing a total of thirty composite beams, all having a square cross-section of 100x100 mm and 1200 mm length. Fig. (**9**) shows the specimen's cross-section.

All specimens were considered as simply supported beams tested under Two-point loading test configuration using a 700 kN capacity MFL Prüf-systeme Universal Testing Machine. Fig. (**10**) shows the test setup. The deflection at the mid span and the applying load locations was measured using three LVDT devices with an accuracy of 0.01 mm. The deflection was measured at 10 kN intervals until failure.
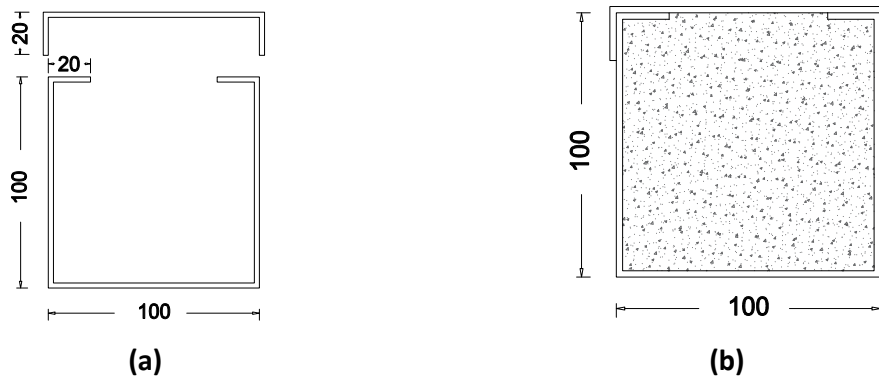

Fig. (9). Composite beam cross-section; (**a**) steel tube; (**b**) composite beam.
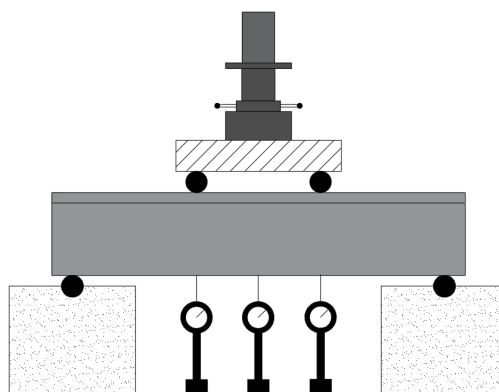

Fig. (10). Test setup.

4. THEORETICAL STUDY USING FINITE ELEMENT ANALYSIS (FEA)

A finite model was adopted using Abaqus software to calculate the flexural capacity of CFT based on the material properties defined in the previous section.

4.1. Parts

The composite beams were constructed using two solid homogeneous parts - the steel tube and concrete infill. Discrete rigid rods were defined to simulate the supports and to apply the experimental displacement to the beams.

4.2. Material Models

Steel was defined as elastic-plastic material, while Tsai's equations were used to simulate the compressive and tensile behavior of concrete [32] Fig. (**11**) illustrates the stress-strain diagrams used for concrete.

4.3. Meshing

A sensitivity analysis was performed with different seeds sizes (50, 30, and 25 mm) and mesh shapes (hexahedral and wedge shapes) to obtain the most accurate results with the least computational time. The best results were recorded using 30 mm mesh size and hexahedral shape; thus, this mesh was approved to continue the analysis. All parts were meshed prior to the assembly of the beams.

4.4. Interactions

General contact with hard contact properties and 0.3 friction coefficient was defined between the beam and the steel rods that were used to induce the deflection to the beam as shown in Fig. (**12**), while a cohesive property was defined between the steel inner face and the concrete outer face based on the tensile stress of each mix defined in the Materials section.

4.5. Boundary Conditions and Test Setup

The supports were defined as pin supports to simulate the actual setup. A displacement control analysis was performed by applying the experimental displacement to the composite beams using two discrete rigid rods in a dynamic explicit step. The two rods were prohibited from translating in any direction except for the direction of the displacement (U2).
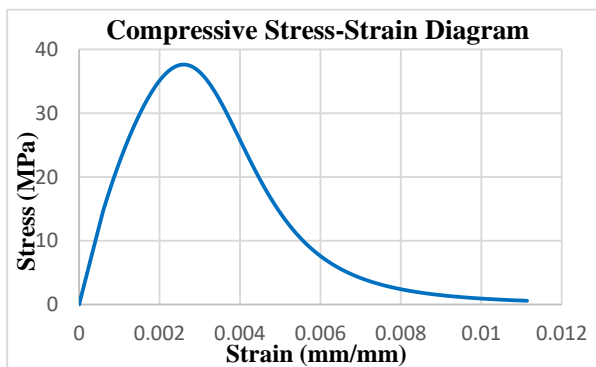
a) Compressive stress-strain diagram for 100%NA   b) Tensile stress-strain diagram for 100%NA
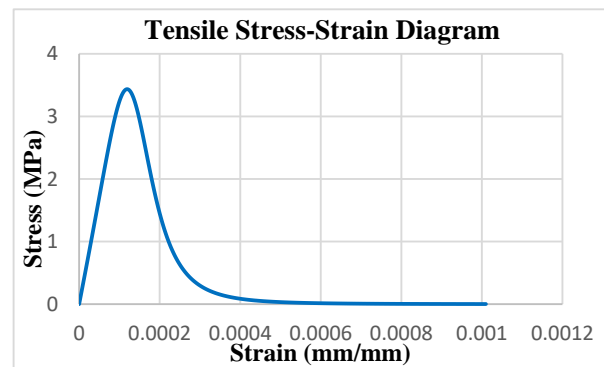
Fig. (11). Stress-strain diagrams of concrete.

Fig. (12). Finite element model.

a) Deflected Shape   (b) Concrete Core Cracks

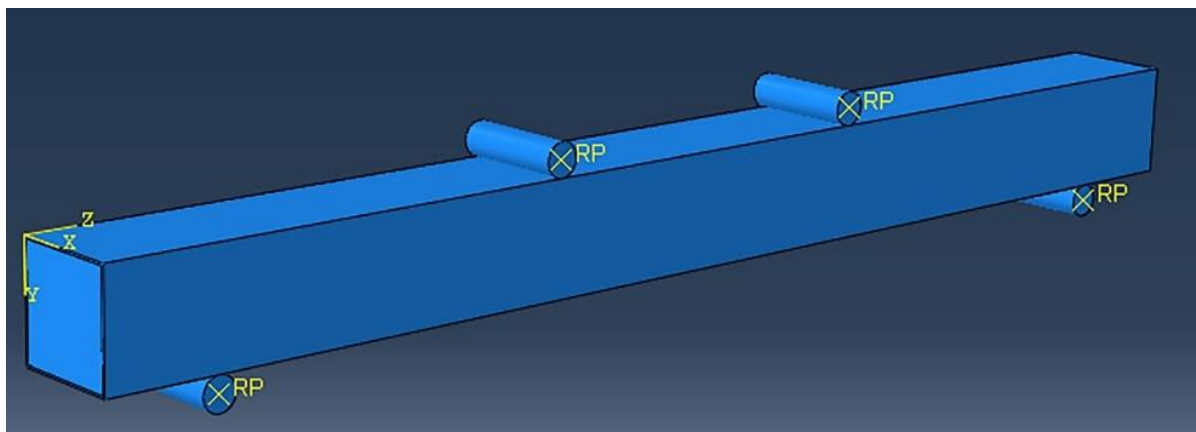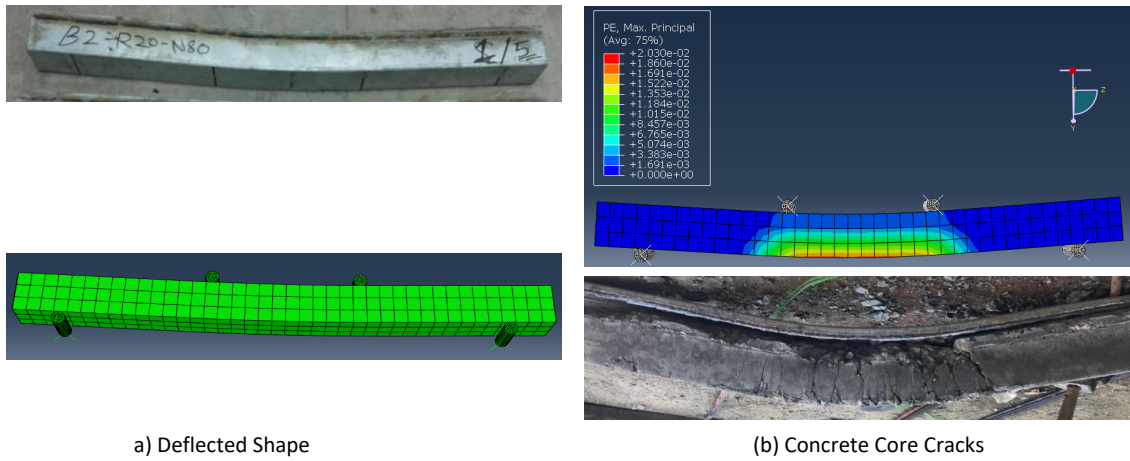**Fig. (13).** Comparison between abaqus and the experimental results.

4.6. Abaqus Results

The calibration of the model took place by comparing the deflected shape of beams, concrete core cracks at failure, and the load-deflection behavior. The deflected shape of beams and the cracks in concrete agreed well with the experimental results as shown in Fig. (**13**).

The load-deflection behavior obtained from Abaqus was also compared with the experimental behavior of all beams and the results are illustrated in Fig. (**14**).

5. RESULTS

The theoretical capacities were calculated according to the above-mentioned codes and compared with the experimental and finite element analysis results. All results are illustrated in Tables **2** and **3** for 2 mm and 2.4 mm steel tubes, respectively.

Table 2. Comparison between experimental and theoretical capacities of composite beams with 2 mm steel thickness.

Sample	M_{uexp} [23]	ACI 318-19 [24]		EC4 [25]		ANSI/AISC 360-16 [26]		AISC-LRFD [27]		AIJ [28]		BS 5400-5 with γ_{mc} and γ_{ms} [29]		BS 5400-5 without γ_{mc} and γ_{ms} [29]		RPT [30]		CoPHK [31]		Han [5]		FEA Model	
		M_{ACI}	M_{ACI}/M_{ue}	M_{EC4}	M_{EC4}/M_{ue}	M_{ANSI}	M_{ANSI}/M_{ue}	M_{AISC}	M_{AISC}/M_{ue}	M_{AIJ}	M_{AIJ}/M_{ue}	M_{BS}	M_{BS}/M_{ue}	M_{BS}	M_{BS}/M_{ue}	M_{RPT}	M_{RPT}/M_{ue}	M_{CoPHK}	M_{CoPHK}/M_{ue}	M_{Han}	M_{Han}/M_{ue}	M_{FE}	M_{FE}/M_{ue}
B2 – N100	14.48	13.50	0.932	10.28	0.710	11.04	0.762	9.66	0.667	9.66	0.667	7.67	0.530	8.83	0.610	10.49	0.724	11.02	0.761	10.30	0.711	11.71	0.808
B2 – R20 – N80	12.18	13.30	1.092	10.24	0.841	11.03	0.906	9.66	0.793	9.66	0.793	7.67	0.630	8.83	0.725	10.45	0.858	11.02	0.905	10.06	0.826	12.13	0.996
B2 – R40 – N60	11.75	13.16	1.120	10.21	0.869	11.03	0.939	9.66	0.822	9.66	0.822	7.67	0.652	8.82	0.751	10.41	0.886	11.01	0.937	9.92	0.844	11.88	1.011
B2 – R60 – N40	11.58	13.21	1.141	10.22	0.883	11.03	0.953	9.66	0.834	9.66	0.834	7.67	0.662	8.83	0.762	10.42	0.900	11.02	0.951	9.96	0.860	11.70	1.010
B2 – R80 – N20	11.75	13.12	1.116	10.2	0.868	11.03	0.939	9.66	0.822	9.66	0.822	7.67	0.652	8.82	0.751	10.4	0.885	11.01	0.937	9.87	0.840	11.51	0.979
B2 – R100	10.98	12.77	1.163	10.13	0.923	11.02	1.004	9.66	0.880	9.66	0.880	7.66	0.698	8.82	0.803	10.25	0.934	11.01	1.002	9.58	0.873	11.60	1.057
B2 – P20 – N80	11.3	13.12	1.161	10.2	0.903	11.03	0.976	9.66	0.855	9.66	0.855	7.67	0.678	8.82	0.781	10.4	0.920	11.01	0.975	9.87	0.873	11.10	0.983
B2 – P40 – N60	10.91	13.07	1.198	10.19	0.934	11.03	1.011	9.66	0.885	9.66	0.885	7.67	0.703	8.82	0.809	10.39	0.952	11.01	1.009	9.83	0.901	11.37	1.042
B2 – P60 – N40	10.93	13.07	1.196	10.19	0.932	11.03	1.009	9.66	0.884	9.66	0.884	7.67	0.701	8.82	0.807	10.39	0.951	11.01	1.008	9.83	0.899	11.04	1.010
B2 – R20 – P80	11.69	12.89	1.103	10.16	0.869	11.03	0.943	9.66	0.826	9.66	0.826	7.66	0.655	8.82	0.754	10.28	0.879	11.01	0.942	9.67	0.828	11.77	1.007
B2 – R40 – P60	12.28	12.82	1.044	10.14	0.826	11.02	0.898	9.66	0.787	9.66	0.787	7.66	0.624	8.82	0.718	10.27	0.836	11.01	0.896	9.62	0.783	11.57	0.943
B2 – R60 – P40	12.28	12.82	1.044	10.15	0.827	11.02	0.898	9.66	0.787	9.66	0.787	7.66	0.624	8.82	0.718	10.27	0.836	11.01	0.896	9.62	0.784	12.05	0.981
B2 – R80 – P20	12.6	13.11	1.040	10.2	0.810	11.03	0.875	9.66	0.767	9.66	0.767	7.67	0.608	8.82	0.700	10.4	0.825	11.01	0.874	9.86	0.783	11.80	0.937
Mean			1.104		0.861		0.932		0.816		0.816		0.648		0.745		0.876		0.930		0.831		0.982

Sample	M_{uexp} [23]	ACI 318-19 [24]		EC4 [25]		ANSI/AISC 360-16 [26]		AISC-LRFD [27]		AIJ [28]		BS 5400-5 with γ_{mc} and γ_{ms} [29]		BS 5400-5 without γ_{mc} and γ_{ms} [29]		RPT [30]		CoPHK [31]		Han [5]		FEA Model	
		M_{ACI}	M_{ACI}/M_{ue}	M_{EC4}	M_{EC4}/M_{ue}	M_{ANSI}	M_{ANSI}/M_{ue}	M_{AISC}	M_{AISC}/M_{ue}	M_{AIJ}	M_{AIJ}/M_{ue}	M_{BS}	M_{BS}/M_{ue}	M_{BS}	M_{BS}/M_{ue}	M_{RPT}	M_{RPT}/M_{ue}	M_{CoPHK}	M_{CoPHK}/M_{ue}	M_{Han}	M_{Han}/M_{ue}	M_{FE}	M_{FE}/M_{ue}
Coefficient of variation		0.065		0.068		0.070		0.070		0.070		0.070		0.070		0.068		0.070		0.063		0.061	
Reduction Percent		-10.4		13.9		6.8		18.4		18.4		35.2		25.5		12.4		7.0		16.9		1.8	

Fig. 16 contd.....

B2-R20-P80

B2-R60-P40

B2-P60-N40

B2-R40-P60

B2-R80-P20

B2.4-N100

B2.4-R20-N80

B2.4-R40-N60
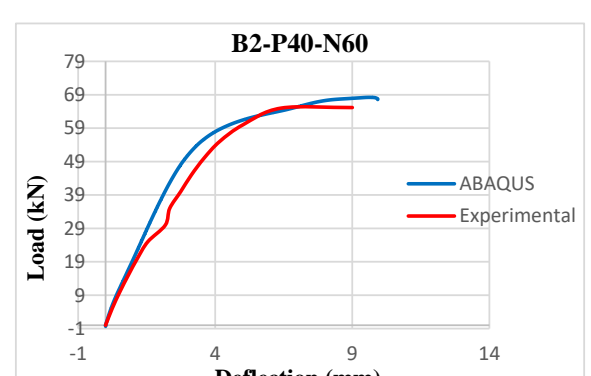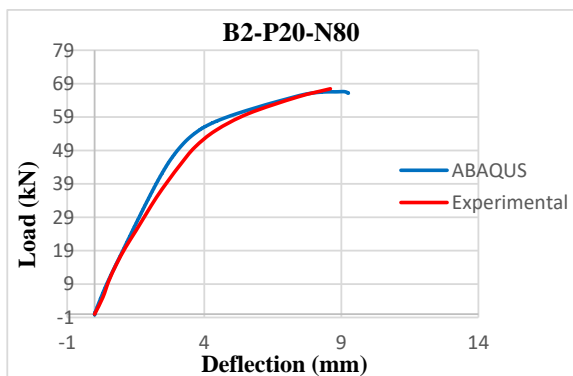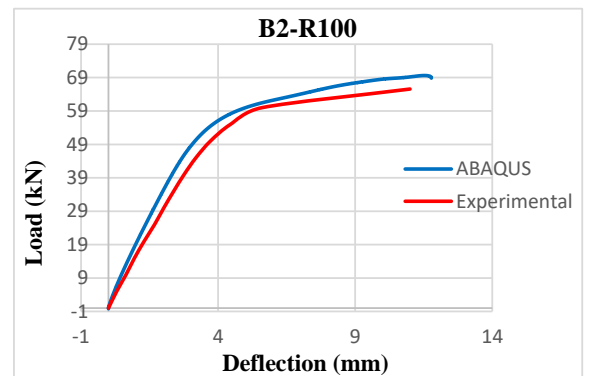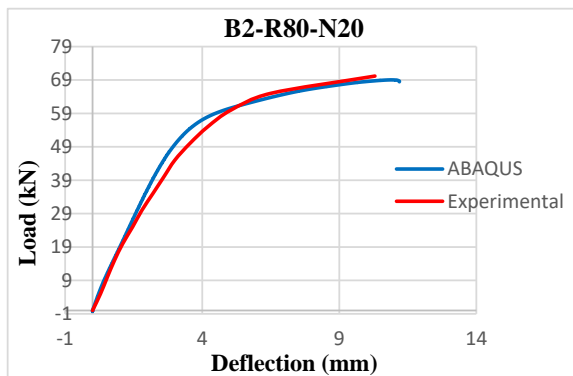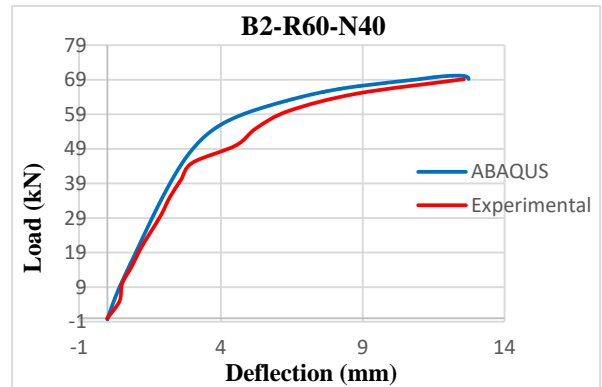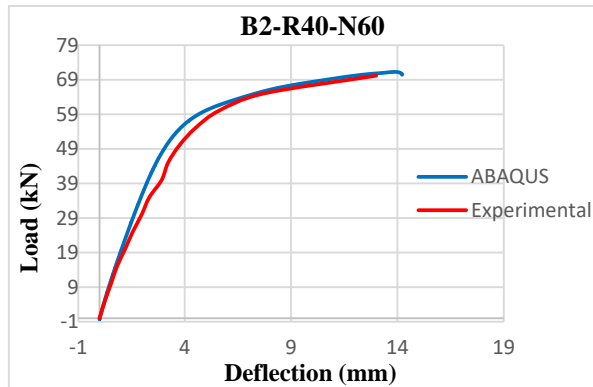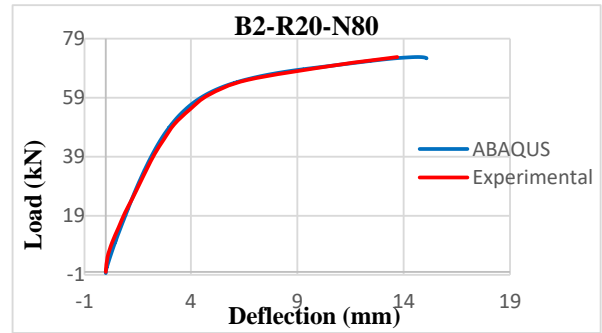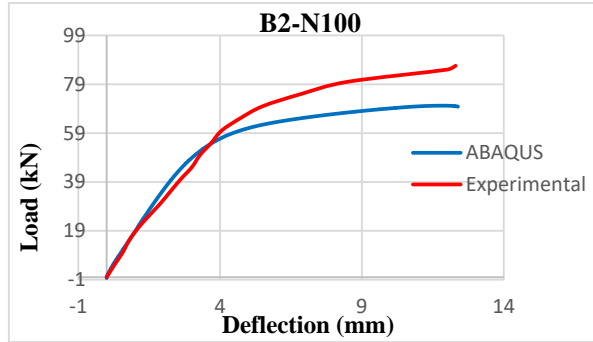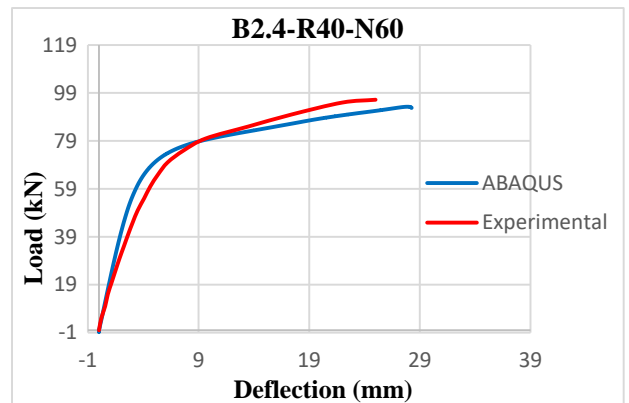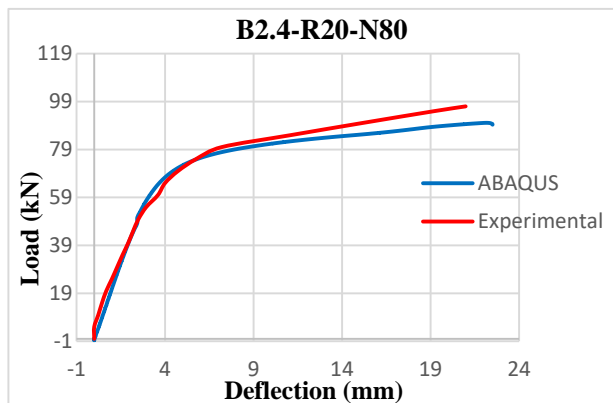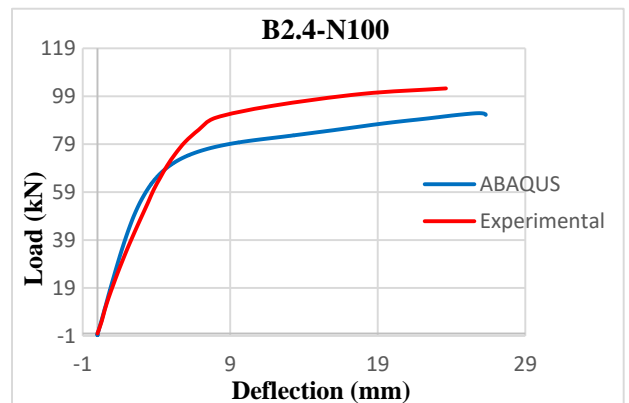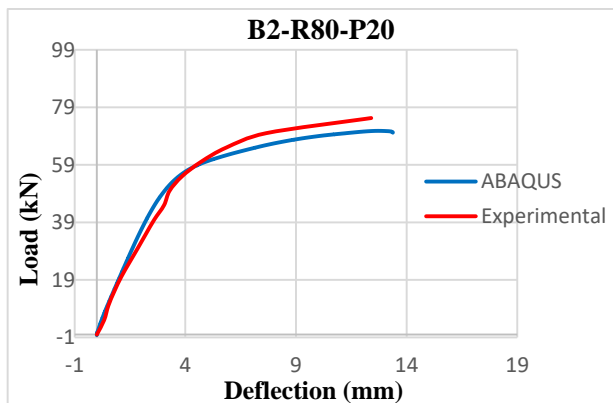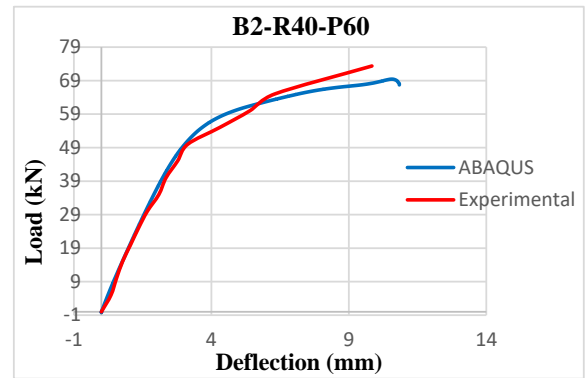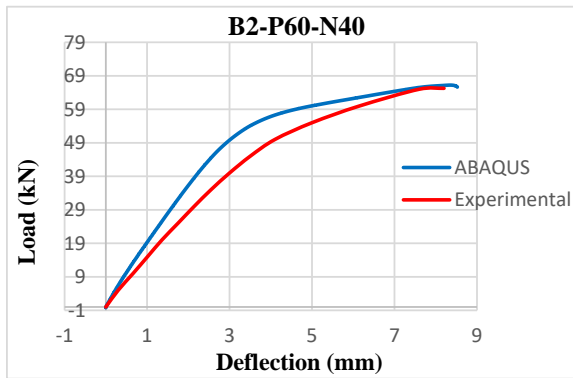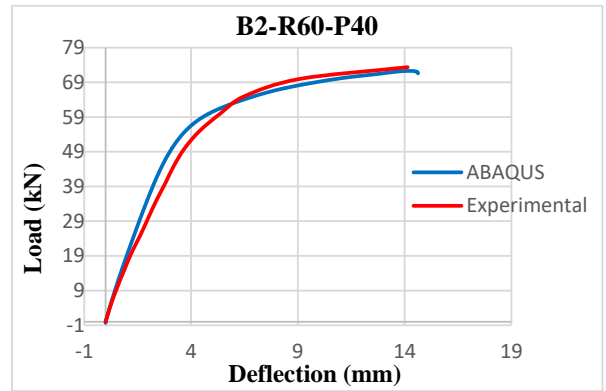
Fig. 16 contd.....

Fig. (14). Comparison between the experimental and abaqus load-deflection behavior.

Table 3. Comparison between experimental and theoretical capacities of composite beams with 2.4 mm steel thickness.

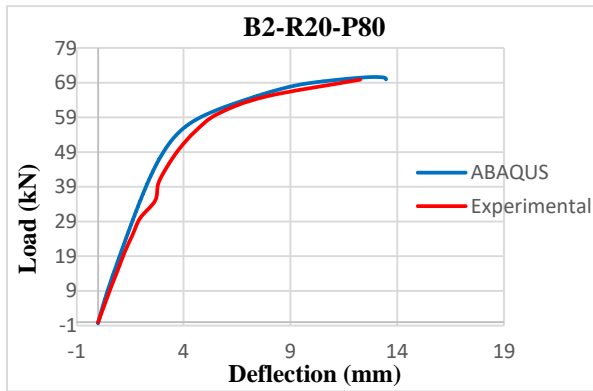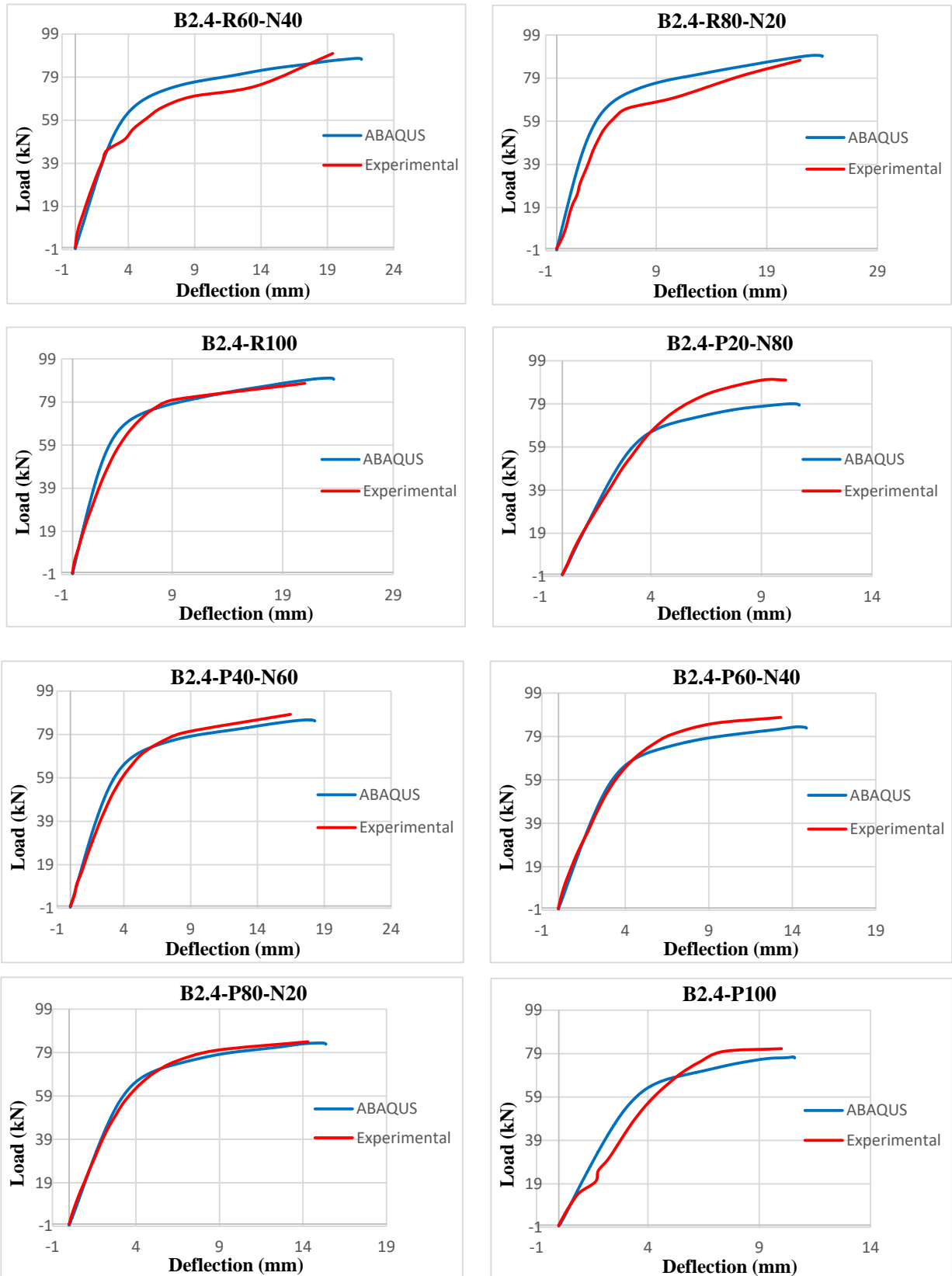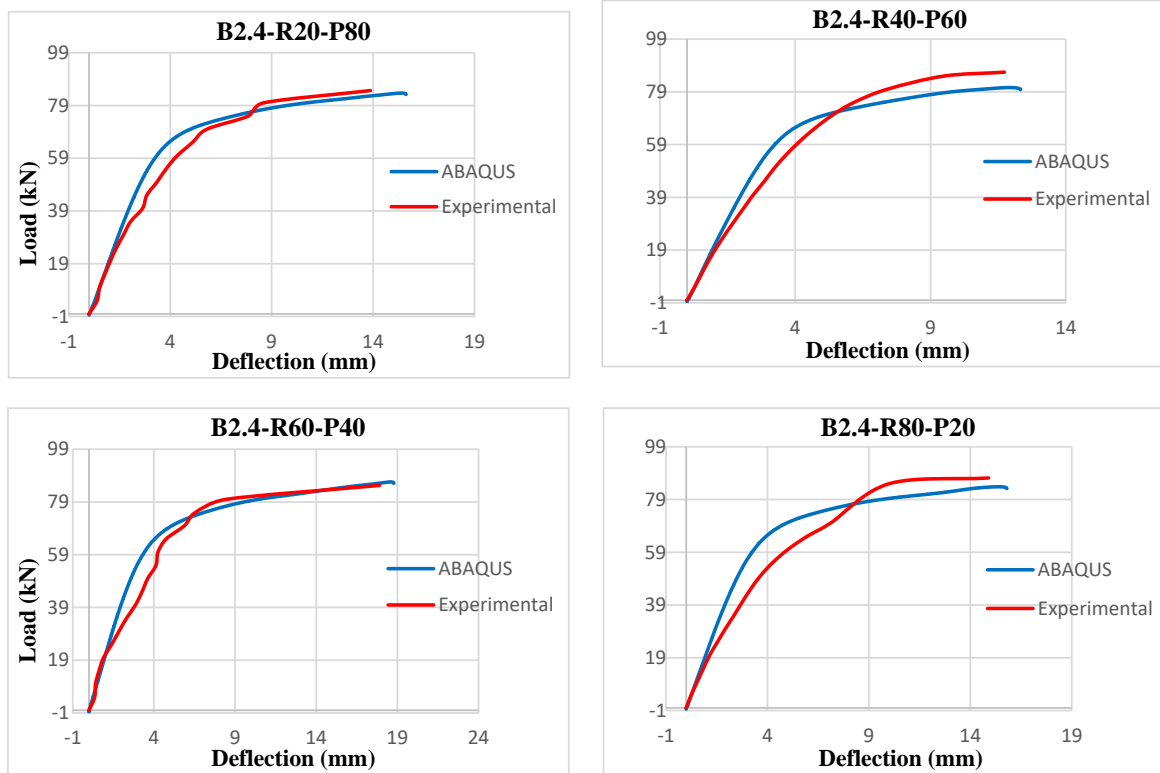| Sample	M_{uexp} [23]	ACI 318-19 [24]		EC4 [25]		ANSI/AISC 360-16 [26]		AISC-LRFD [27]		AIJ [28]		BS 5400-5 with γ_{mc} and γ_{ms} [29]		BS 5400-5 without γ_{mc} and γ_{ms} [29]		RPT [30]		CoPHK [31]		Han [5]		FEA Model	
		M_{ACI}	M_{ACI}/M_{ue}	M_{EC4}	M_{EC4}/M_{ue}	M_{ANSI}	M_{ANSI}/M_{ue}	M_{AISC}	M_{AISC}/M_{ue}	M_{AIJ}	M_{AIJ}/M_{ue}	M_{BS}	M_{BS}/M_{ue}	M_{BS}	M_{BS}/M_{ue}	M_{RPT}	M_{RPT}/M_{ue}	M_{CoPHK}	M_{CoPHK}/M_{ue}	M_{Han}	M_{Han}/M_{ue}	M_{FE}	M_{FE}/M_{ue}
B2.4 – N100	17.10	15.87	0.928	12.22	0.715	13.19	0.771	11.58	0.677	11.58	0.677	9.16	0.536	10.55	0.617	12.45	0.728	13.17	0.770	12.15	0.711	15.32	0.896
B2.4 – R20 – N80	16.22	15.65	0.965	12.18	0.751	13.18	0.813	11.58	0.714	11.58	0.714	9.16	0.565	10.54	0.650	12.3	0.758	13.16	0.811	11.92	0.735	15.02	0.926
B2.4 – R40 – N60	16.08	15.49	0.963	12.15	0.756	13.18	0.819	11.58	0.720	11.58	0.720	9.16	0.570	10.54	0.656	12.27	0.763	13.16	0.818	11.79	0.733	15.54	0.966
B2.4 – R60 – N40	15.05	15.54	1.033	12.16	0.808	13.18	0.876	11.58	0.769	11.58	0.769	9.16	0.609	10.54	0.700	12.28	0.816	13.16	0.874	11.83	0.786	14.62	0.971
B2.4 – R80 – N20	14.60	15.44	1.058	12.14	0.832	13.18	0.903	11.58	0.793	11.58	0.793	9.16	0.627	10.54	0.722	12.25	0.839	13.16	0.901	11.74	0.804	14.93	1.023
B2.4 – R100	14.66	15.06	1.027	12.06	0.823	13.17	0.898	11.58	0.790	11.58	0.790	9.15	0.624	10.53	0.718	12.16	0.829	13.15	0.897	11.50	0.784	15.01	1.024
B2.4 – P20 – N80	15.21	15.44	1.015	12.14	0.798	13.18	0.866	11.58	0.761	11.58	0.761	9.16	0.602	10.54	0.693	12.25	0.805	13.16	0.865	11.74	0.772	13.18	0.866
B2.4 – P40 – N60	14.76	15.39	1.042	12.13	0.822	13.17	0.892	11.58	0.784	11.58	0.784	9.16	0.620	10.54	0.714	12.24	0.829	13.16	0.891	11.70	0.793	14.29	0.968
B2.4 – P60 – N40	14.68	15.39	1.048	12.13	0.826	13.17	0.897	11.58	0.789	11.58	0.789	9.16	0.624	10.54	0.718	12.24	0.834	13.16	0.896	11.70	0.797	13.91	0.947
B2.4 – P80 – N20	14.05	15.29	1.089	12.11	0.862	13.17	0.938	11.58	0.824	11.58	0.824	9.16	0.652	10.54	0.750	12.22	0.870	13.15	0.936	11.64	0.828	13.90	0.990
B2.4 – P100	13.60	15.18	1.117	12.09	0.889	13.17	0.969	11.58	0.852	11.58	0.852	9.15	0.673	10.54	0.775	12.19	0.897	13.15	0.967	11.56	0.851	12.91	0.950
B2.4 – R20 – P80	14.16	15.19	1.073	12.09	0.854	13.17	0.930	11.58	0.818	11.58	0.818	9.15	0.646	10.54	0.744	12.19	0.861	13.15	0.929	11.57	0.817	13.95	0.985

Sample	M_{uexp} [23]	ACI 318-19 [24]		EC4 [25]		ANSI/AISC 360-16 [26]		AISC-LRFD [27]		AIJ [28]		BS 5400-5 with γ_{mc} and γ_{ms} [29]		BS 5400-5 without γ_{mc} and γ_{ms} [29]		RPT [30]		CoPHK [31]		Han [5]		FEA Model	
		M_{ACI}	M_{ACI}/M_{ue}	M_{EC4}	M_{EC4}/M_{ue}	M_{ANSI}	M_{ANSI}/M_{ue}	M_{AISC}	M_{AISC}/M_{ue}	M_{AIJ}	M_{AIJ}/M_{ue}	M_{BS}	M_{BS}/M_{ue}	M_{BS}	M_{BS}/M_{ue}	M_{RPT}	M_{RPT}/M_{ue}	M_{CoPHK}	M_{CoPHK}/M_{ue}	M_{Han}	M_{Han}/M_{ue}	M_{FE}	M_{FE}/M_{ue}
B2.4 – R40 – P60	14.46	15.11	1.045	12.07	0.835	13.17	0.910	11.58	0.801	11.58	0.801	9.15	0.633	10.53	0.728	12.17	0.841	13.15	0.909	11.53	0.797	13.44	0.929
B2.4 – R60 – P40	14.26	15.12	1.060	12.07	0.846	13.17	0.923	11.58	0.812	11.58	0.812	9.15	0.642	10.53	0.739	12.17	0.853	13.15	0.922	11.53	0.808	14.43	1.012
B2.4 – R80 – P20	14.58	15.43	1.058	12.4	0.851	13.18	0.904	11.58	0.794	11.58	0.794	9.16	0.628	10.54	0.723	12.25	0.840	13.16	0.902	11.73	0.805	13.97	0.958
Mean			1.035		0.818		0.887		0.780		0.780		0.617		0.710		0.824		0.886		0.788		0.961
Coefficient of variation			0.047		0.055		0.057		0.057		0.057		0.057		0.057		0.053		0.124		0.046		0.045
Reduction Percent			-3.5		18.2		11.3		22.0		22.0		38.3		29.0		17.6		11.4		21.2		3.9

Abbreviations:

B2, B2.4: composite beam of 2 mm and 2.4 mm steel thickness, respectively.

N: Natural aggregate concrete (NA).

R: Recycled concrete aggregate (RCA).

P: Recycled asphalt pavement aggregate (RAP).

6. DISCUSSION

For both 2 mm and 2.4 mm steel thicknesses, not all codes were conservative in predicting the theoretical capacity. The ACI 318-19 [24] overestimated the capacity by about 10% and 4% for 2 mm and 2.4 mm steel, respectively. It gave higher results of 12 specimens out of 13 for 2 mm steel and 12 specimens out of 15 for 2.4 mm steel. Fig. (**15**) shows a comparison of results for both steel thicknesses.
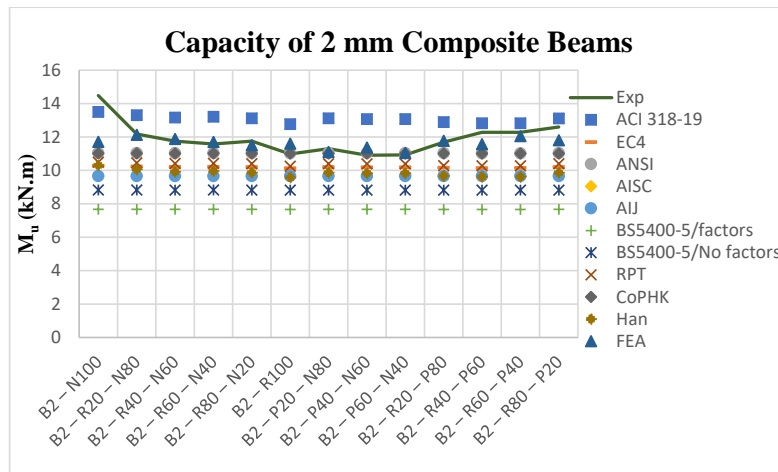
(a) 2 mm Composite Beams Capacity
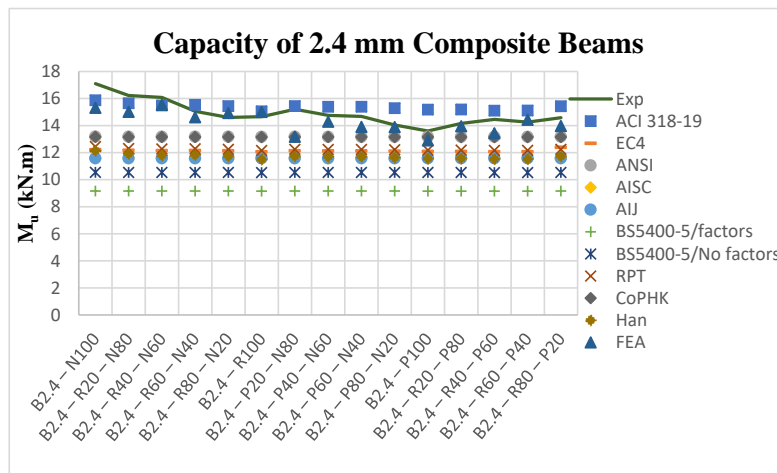
(b) 2.4 mm Composite Beams Capacity

Fig. (15). Comparison of capacities for 2 and 2.4 mm composite beams

For 2 mm steel, the ANSI/AISC 360-16 [26] and CoPHK [31] provided conservative and the most accurate results among all codes with a reduction percent of about 7% and a coefficient of variation of 0.070. Both codes predicted the exact capacities of 3 specimens, namely, B2 – R100; B2 – P40 – N60; and B2 – P60 – N40, while the calculated moments of other samples were smaller than the experimental ones. The RPT [30], EC4 [25], and the proposed method by Han [5] provided good estimation of moments, but they underestimated the capacities by about 12%, 14%, and 17%, respectively.

The AISC-LRFD [27] and AIJ [28] used the same approach to calculate the bending moments of CFT. Both codes provided conservative results with a reduction percent of about 18%. Finally, the theoretical moments were calculated according to the BS 5400-5 [29] twice, one time with γ_{mc} and γ_{ms} having their values as defined by the code and another time taken as unity. In the case where γ_{mc} and γ_{ms} were taken as unity, a 26% reduction percent was recorded, while when their values were under consideration, the highest reduction percent was recorded, which was about 35%.

For 2.4 mm steel tubes, the accuracy of the codes was found to have the same order as the 2 mm steel thickness but with different reduction percent. The lowest reduction was recorded for the ANSI/AISC 360-16 [26] and CoPHK [31] with a value of 11%, followed by the RPT [30] and EC4 [25] with a value of 18%. The proposed method by Han [5] recorded values with 21% reduction percent. Because both the

AISC-LRFD [27] and AIJ [28] used the same assumptions, their values were 22% lower than the experimental ones. Finally, the BS 5400-5 [29] recorded capacities with 29% reduction when γ_{mc} and γ_{ms} were taken as unity and 38% lower than the experimental values when γ_{mc} and γ_{ms} were considered.

Another aspect was used to assess the effect of the compressive strength of concrete on the results obtained by the previous methods [32 - 34]. Tables **4** and **5** illustrate the reduction in the flexural capacity obtained from previous equations compared to the actual reduction in the experimental results according to the reduction of compressive strength for 2 and 2.4 mm steel thicknesses, respectively. Since the AISC-LRFD [27] and AIJ [28] codes do not consider the concrete core in the calculations, they were not included in the comparison. It can be seen from the tables that the flexural capacity of all composite beams was reduced due to the reduction in the compressive strength of concrete. The capacity of composite beams filled with recycled aggregates was (13%-25%) and (5%-20%) lower than the composite beams filled with normal concrete for 2 and 2.4 mm beams, respectively. However, the reduction in flexural strength according to the ANSI/AISC 360-16 [26], BS 5400-5 [29], and CoPHK [31] was 0% for all composite beams, while for the ACI 318-19 [24], EC4 [25], RPT [30], Han [5], and the Abaqus results were negligible, with the highest reduction recorded for the Abaqus results. This does not agree well with the experimental results.

Table 4. Reduction in the flexural capacities due to f'$_c$ reduction for 2 mm steel composite beams.

	f'$_c$ (MPa)	M$_u$ (kN.m)	Reduction in f'$_c$	Reduction in M$_u$	M$_{ACI}$	M$_{EC4}$	M$_{ANSI}$	M$_{BS}$/ factors	M$_{BS}$/no factors	M$_{RPT}$	M$_{CoPHK}$	M$_{Han}$	M$_{FE}$
B2 – N100	37.62	14.48	-	-	-	-	-	-	-	-	-	-	-
B2 – R20 – N80	32.36	12.18	14%	16%	1%	0%	0%	0%	0%	0%	0%	2%	-4%
B2 – R40 – N60	29.04	11.75	23%	19%	3%	1%	0%	0%	0%	1%	0%	4%	-1%
B2 – R60 – N40	30.09	11.58	20%	20%	2%	1%	0%	0%	0%	1%	0%	3%	0%
B2 – R80 – N20	27.95	11.75	26%	19%	3%	1%	0%	0%	0%	1%	0%	4%	2%
B2 – R100	20.83	10.98	45%	24%	5%	1%	0%	0%	0%	2%	0%	7%	1%
B2 – P20 – N80	27.96	11.30	26%	22%	3%	1%	0%	0%	0%	1%	0%	4%	5%
B2 – P40 – N60	26.94	10.91	28%	25%	3%	1%	0%	0%	0%	1%	0%	5%	3%
B2 – P60 – N40	26.96	10.93	28%	25%	3%	1%	0%	0%	0%	1%	0%	5%	6%
B2 – P80 – N20	25.14	-	-	-	-	-	-	-	-	-	-	-	-
B2 – P100	23.02	-	-	-	-	-	-	-	-	-	-	-	-
B2 – R20 – P80	23.24	11.69	38%	19%	5%	1%	0%	0%	0%	2%	0%	6%	-1%
B2 – R40 – P60	21.81	12.28	42%	15%	5%	1%	0%	0%	0%	2%	0%	7%	1%
B2 – R60 – P40	21.89	12.28	42%	15%	5%	1%	0%	0%	0%	2%	0%	7%	-3%
B2 – R80 – P20	27.74	12.60	26%	13%	3%	1%	0%	0%	0%	1%	0%	4%	-1%

Table 5. Reduction in the flexural capacities due to f'$_c$ reduction for 2.4 mm steel composite beams.

	f'$_c$ (MPa)	M$_u$ (kN.m)	Reduction in f'$_c$	Reduction in M$_u$	M$_{ACI}$	M$_{EC4}$	M$_{ANSI}$	M$_{BS}$/ factors	M$_{BS}$/no factors	M$_{RPT}$	M$_{CoPHK}$	M$_{Han}$	M$_{FE}$
B2.4 – N100	37.62	17.10	-	-	-	-	-	-	-	-	-	-	-
B2.4 – R20 – N80	32.36	16.22	14%	5%	1%	0%	0%	0%	0%	1%	0%	2%	2%
B2.4 – R40 – N60	29.04	16.08	23%	6%	2%	1%	0%	0%	0%	1%	0%	3%	-1%
B2.4 – R60 – N40	30.09	15.05	20%	12%	2%	0%	0%	0%	0%	1%	0%	3%	5%

	f'_c (MPa)	M_u (kN.m)	Reduction in f'_c	Reduction in M_u	M_{ACI}	M_{EC4}	M_{ANSI}	M_{BS}/factors	M_{BS}/no factors	M_{RPT}	M_{CoPHK}	M_{Han}	M_{FE}
B2.4 – R80 – N20	27.95	14.60	26%	15%	3%	1%	0%	0%	0%	2%	0%	3%	3%
B2.4 – R100	20.83	14.66	45%	14%	5%	1%	0%	0%	0%	2%	0%	5%	2%
B2.4 – P20 – N80	27.96	15.21	26%	11%	3%	1%	0%	0%	0%	2%	0%	3%	14%
B2.4 – P40 – N60	26.94	14.76	28%	14%	3%	1%	0%	0%	0%	2%	0%	4%	7%
B2.4 – P60 – N40	26.96	14.68	28%	14%	3%	1%	0%	0%	0%	2%	0%	4%	9%
B2.4 – P80 – N20	25.14	14.05	33%	18%	4%	1%	0%	0%	0%	2%	0%	4%	9%
B2.4 – P100	23.02	13.60	39%	20%	4%	1%	0%	0%	0%	2%	0%	5%	16%
B2.4 – R20 – P80	23.24	14.16	38%	17%	4%	1%	0%	0%	0%	2%	0%	5%	9%
B2.4 – R40 – P60	21.81	14.46	42%	15%	5%	1%	0%	0%	0%	2%	0%	5%	12%
B2.4 – R60 – P40	21.89	14.26	42%	17%	5%	1%	0%	0%	0%	2%	0%	5%	6%
B2.4 – R80 – P20	27.74	14.58	26%	15%	3%	-1%	0%	0%	0%	2%	0%	3%	9%

According to the literature review mentioned in this current research, Han *et al.* [5] concluded that the EC4 gave the best conservative estimation among all considered codes with the highest accuracy. It gave an average of 14% lower than the experimental results, while the LRFD (1999) and AIJ (1997) provided a section capacity of about 25% lower than the tested values, and this order is consistent with the results of this study except for the BS5400. According to Han *et al.* [5], the BS5400 [29] provided results higher than the AISC-LRFD [27] and AIJ [28], which is not the case of this study unless all factors were taken as unity.

Furthermore, it was highlighted that several codes could be extended to get a conservative estimation for different conditions such as new slenderness range [9], elliptical shape [17], and high tensile steel with ultra-high concrete strength [20].

For the cases where steel corrosion is a key factor [4], it is safe to use different codes such as DB36/J001-2007 (2007), AIJ (1997), and EN 1994-1-1:2004 (2004) to estimate the moment capacity of beams, taking into consideration the reduction in yield strength of the outer steel tube, while for the GB 50936-2014 (2014), the loss in wall thickness should also be considered to provide a conservative estimation.

Other code provisions such as CIDECT were also considered in the literature. Soundararajan and Shanmugasundaram [3], Elchalakani *et al.* [9], and Wheeler and Bridge [13] used the CIDECT standard to calculate the flexural capacity of CFTs and found that CIDECT generally provided conservative results.

In recent research, computer technologies have been playing an important role in capacity calculation and behavior simulation. The finite element analysis was used to predict the performance of CFT, and a very good agreement was found between the models and the experimental results, according to the literature using Abaqus [23, 6, 7] and ANSYS [22]. In this study, the flexural capacity of CFT was calculated according to El-Nimri *et al'* s [23] model and the results were found to record the lowest reduction percent among all codes. For 2 mm and 2.4 mm steel, the capacities were about 2% and 4% lower than the experimental results, respectively.

CONCLUSION

From the results of this study, as well as the past research, the following conclusions can be reached:

(1) There is a lack of information and tests on the flexural behavior of concrete-filled tubes.

(2) All available codes can be used to predict the moment capacity of CFT regardless of the steel type and concrete infill used, as they gave conservative results if used according to the limitations mentioned in each code, except for the ACI 318-19, where it provided results higher than the experimental ones by (3%-10%)

(3) The ANSI/AISC 360-16 and CoPHK have proven that they are the most accurate methods to calculate the flexural capacity of CFTs.

(4) The RPT, EC4, the proposed method by Han [5], AISC-LRFD, AIJ, and BS5400-5 can be used to conservatively predict the flexural capacity of CFTs, with the RPT providing the highest accuracy and BS5400-5 providing the lowest one.

(5) The flexural capacity of composite beams decreased with the decrease of the concrete compressive strength because of the use of recycled aggregates; however, the reduction in capacity recorded according to the equations in the literature was negligible.

(6) All code provisions can be extended to cover further cases such as different steel tube shapes, steel corrosion, new slenderness ranges, and high tensile steel with ultra-high concrete strength by considering specific factors.

(7) The finite element analysis results were found to compare favorably with the experimental ones, where they recorded the lowest reduction in capacity for both steel thicknesses.

CONSENT FOR PUBLICATION

Not applicable.

AVAILABILITY OF DATA AND MATERIALS

The data associated with this paper are available upon request.

CONFLICT OF INTEREST

The authors declare no conflict of interest, financial or otherwise.

ACKNOWLEDGEMENTS

Declared none.

REFERENCES

[1]   L.H. Han, H.Y. Guo, and L.Z. Xiao, "Behavior and calculation on concrete-filled steel CHS (Circular Hollow Section) beam-columns", *Steel Compos. Struct.,* vol. 4, no. 3, pp. 169-188, 2004.
[http://dx.doi.org/10.12989/scs.2004.4.3.169]

[2]   Y.M. Hunaiti, "Strength of composite sections with foamed and lightweight aggregate concrete", *J. Mater. Civ. Eng.,* vol. 9, no. 2, pp. 58-61, 1997.
[http://dx.doi.org/10.1061/(ASCE)0899-1561(1997)9:2(58)]

[3]   A. Soundararajan, and K. Shanmugasundaram, "Flexural behaviour of concrete-filled steel hollow sections beams", *J. Civ. Eng. Manag.,* vol. 14, no. 2, pp. 107-114, 2008.
[http://dx.doi.org/10.3846/1392-3730.2008.14.5]

[4]   L. Xie, M. Chen, W. Sun, F. Yuan, and H. Huang, "Behaviour of concrete-filled steel tubular members under pure bending and acid rain attack: Test simulation", *Adv. Struct. Eng.,* vol. 22, no. 1, pp. 240-253, 2019.
[http://dx.doi.org/10.1177/1369433218783323]

[5]   L.H. Han, "Flexural behaviour of concrete-filled steel tubes", *J. Construct. Steel Res.,* vol. 60, no. 2, pp. 313-337, 2004.
[http://dx.doi.org/10.1016/j.jcsr.2003.08.009]

[6]   H. Lu, L.H. Han, and X.L. Zhao, "Analytical behavior of circular concrete-filled thin-walled steel tubes subjected to bending", *Thin-walled Struct.,* vol. 47, no. 3, pp. 346-358, 2009.
[http://dx.doi.org/10.1016/j.tws.2008.07.004]

[7]   S. Al-Obaidi, T. Salim, and S.A. Hemzah, "Flexural behavior of concrete filled steel tube composite with different concrete compressive strength", *Int Journal Civil Eng Tech,* vol. 9, no. 7, pp. 824-832, 2018.

[8]   M. Lee, and T. Kang, *Computation for flexural strength of circular concrete filled tube..* n.d.

[9]   M. Elchalakani, X.L. Zhao, and R.H. Grzebieta, "Concrete-filled circular steel tubes subjected to pure bending", *J. Construct. Steel Res.,* vol. 57, no. 11, pp. 1141-1168, 2001.
[http://dx.doi.org/10.1016/S0143-974X(01)00035-9]

[10]   I. M. Assi, E. M. Qudeimat, and Y. M. Hunaiti, "Ultimate moment capacity of foamed and lightweight aggregate concrete-filled steel tubes", *Steel Compos Struct,* vol. 3, no. 3, pp. 199-212, .
[http://dx.doi.org/10.12989/scs.2003.3.3.199]

[11]   Y.F. Yang, and L.H. Han, "Compressive and flexural behaviour of recycled aggregate concrete filled steel tubes (RACFST) under short-term loadings", *Steel Compos. Struct.,* vol. 6, no. 3, pp. 257-284, 2006.
[http://dx.doi.org/10.12989/scs.2006.6.3.257]

[12]   L.H. Han, H. Lu, G.H. Yao, and F.Y. Liao, "Further study on the flexural behaviour of concrete-filled steel tubes", *J. Construct. Steel Res.,* vol. 62, no. 6, pp. 554-565, 2006.
[http://dx.doi.org/10.1016/j.jcsr.2005.09.002]

[13]   A. Wheeler, and R. Bridge, "The behaviour of circular concrete-filled thin-walled steel tubes in flexure", *Construction,* pp. 390-401, 2006.

[14]   M. Fong, S.T. Chan, and S.L. Chan, "Capacities of concrete-filled steel beams of unequal double spans by testing and code", *HKIE Transactions Hong Kong Institution of Engineers,* vol. 18, no. 1, pp. 1-5, 2011.
[http://dx.doi.org/10.1080/1023697X.2011.10668217]

[15]   C.W. Roeder, D.E. Lehman, and E. Bishop, "Strength and stiffness of circular concrete-filled tubes", *J. Struct. Eng.,* vol. 136, no. 12, pp. 1545-1553, 2010.
[http://dx.doi.org/10.1061/(ASCE)ST.1943-541X.0000263]

[16]   Y.F. Yang, and G.L. Ma, "Experimental behaviour of recycled aggregate concrete filled stainless steel tube stub columns and beams", *Thin-walled Struct.,* vol. 66, pp. 62-75, 2013.
[http://dx.doi.org/10.1016/j.tws.2013.01.017]

[17]   Q.X. Ren, L.H. Han, D. Lam, and W. Li, "Tests on elliptical concrete filled steel tubular (CFST) beams and columns", *J. Construct. Steel Res.,* vol. 99, pp. 149-160, 2014.
[http://dx.doi.org/10.1016/j.jcsr.2014.03.010]

[18]   K.N. Jyothi, and T. Valsa Ipe, "Performance of infilled cold formed steel channel section beams", *Int. J. Engine Res.,* vol. V4, no. 12, pp. 446-451, 2015.
[http://dx.doi.org/10.17577/IJERTV4IS120523]

[19]   J.M. Flor, R.H. Fakury, R.B. Caldas, F.C. Rodrigues, and A.H.M. Araújo, "Experimental study on the flexural behavior of large-scale rectangular concrete-filled steel tubular beams", *Rev. IBRACON Estrut. Mater.,* vol. 10, no. 4, pp. 895-905, 2017.
[http://dx.doi.org/10.1590/s1983-41952017000400007]

[20]   M.X. Xiong, D.X. Xiong, and J.Y.R. Liew, "Flexural performance of concrete filled tubes with high tensile steel and ultra-high strength concrete", *J. Construct. Steel Res.,* vol. 132, pp. 191-202, 2017.
[http://dx.doi.org/10.1016/j.jcsr.2017.01.017]

[21]   A. Nghiem, T.H.K. Kang, M. Lee, C. Ramseyer, and C.H. Lee, "Flexural testing of circular concrete-filled tubes without axial forces", *ACI Struct. J.,* vol. 115, no. 2, pp. 511-523, 2018.
[http://dx.doi.org/10.14359/51701134]

[22]   M. F. Javed, N. H. Ramli Sulong, N. B. Khan, and S. Kashif, *Finite element analysis of the flexural behavior of square CFST beams at ambient and elevated temperature.,* 2018.
[http://dx.doi.org/10.4995/ASCCS2018.2018.7236]

[23]   R. El-Nimri, M.S. Abdel-Jaber, Y.M. Hunaiti, and M. Abdel-Jaber, "Behavior of light-gauge steel beams filled with recycled concrete", *Magazine of Civil Engineering.,* vol. 101, no. 1, p. 10102, 2021.
[http://dx.doi.org/10.34910/MCE.101.2]

[24]   ACI 319, *318M-19: Building Code Requirements for Reinforced Concrete and Commentary,* 2019.

[25]   Eurocode 4, Design of composite steel and concrete structures, Part1.1: General rules and rules for buildings (together with United Kingdom National Application Document).*DD ENV 1994-1-1:1994,* British Standards Institution: London, 1994.

[26]   AISC, *AISC360/16 Specification for Structural Steel Buildings, an American National Standard,* 2016, p. 612 .

[27]   AISC-LRFD, *Load and resistance factor design specification for structural steel buildings,* 2nd ed American Institute of Steel Construction (AISC): Chicago, U.S.A, 1999.

[28]   AIJ, *Recommendations for design and construction of concrete filled steel tubular structures.,* Architectural Institute of Japan: Tokyo, Japan, 1997.

[29]   British Standard Institute, *BS5400, Part 5.,* Concrete and Composite Bridges: London, U.K., 1979.

[30]   T. Valsa Ipe, H. Sharada Bai, K. Manjula Vani, and M.M.Z. Iqbal, "Flexural behavior of cold-formed steel concrete composite beams", *Steel Compos. Struct.,* vol. 14, no. 2, pp. 105-120, 2013.
[http://dx.doi.org/10.12989/scs.2013.14.2.105]

[31]   *CoPHK, Code of Practice for Structural Use of Steel 2005.,* Buildings Department, the HKSAR Government: Hong Kong, 2005.

[32]   R. Allouzi, A. Alkloub, H. Naghawi, and R. Al-Ajarmeh, "Fracture modeling of concrete in plain and reinforced concrete members", *Int. J. Civ. Eng.,* vol. 17, no. 7, pp. 1029-1042, 2019.
[http://dx.doi.org/10.1007/s40999-018-0353-5]

[33]   R. Montuori, V. Piluso, and A. Tisi, "Ultimate behaviour of FRP wrapped sections under axial force and bending: Influence of stress-strain confinement model", *Compos., Part B Eng.,* vol. 54, no. 1, pp. 85-96, 2013.
[http://dx.doi.org/10.1016/j.compositesb.2013.04.059]

[34]   R. Montuori, V. Piluso, and A. Tisi, "Comparative analysis and critical issues of the main constitutive laws for concrete elements confined with FRP", *Compos., Part B Eng.,* vol. 43, no. 8, pp. 3219-3230, 2012.
[http://dx.doi.org/10.1016/j.compositesb.2012.04.001]